ROCKET INVESTIGATION OF THE MgI and MgII DAYGLOW

James G. Anderson and Charles A. Barth

Department of Astro-Geophysics and
Laboratory for Atmospheric and Space Physics
University of Colorado, Boulder, Colorado 80302

ABSTRACT

The 2800 Å dayglow of ionized magnesium in a sporadic E layer was measured by a rocket borne ultraviolet spectrometer. Because the 2852 Å line of neutral magnesium was less than 10 Rayleighs while the ionized magnesium emission was measured to be 360 Rayleighs, the ratio of Mg^+ to Mg was determined to be greater than 22. A model of the ion chemistry in the sporadic E layer shows that neutral magnesium is ionized predominately by the charge transfer reaction with NO^+ at a rate greater than 7×10^{-11} cm^3 sec^{-1} or 1.5×10^{-9} cm^3 sec^{-1} depending on the role MgO_2^+ plays in the chemistry. In this model, Mg^+ is converted back into Mg by radiative recombination.

Introduction

A great deal has been learned in recent years about the behavior of metallic ions in the E region of the ionosphere using a variety of experimental techniques. In situ measurements using ion mass spectrometers (Istomin, 1963; Narcisi et al., 1967; Narcisi, 1968) with extensive laboratory investigation of ionic reactions (Fehsenfeld et al., 1966; Fehsenfeld et al., 1968; Ferguson et al., 1965; Ferguson and Fehsenfeld, 1968) have been combined with data from radio soundings (McKinley, 1961) and analysis of chemical releases (Rosenberg, 1966) to formulate a general picture of metallic ions.

This paper will discuss the simultaneous observations of Mg and Mg^+ using rocket borne optical techniques in the near ultraviolet. Comment will be confined to a single event characterized by a highly ionized layer generally fitting the description of a sporadic E event. Characteristics of the event such as horizontal variation in the metallic ion density and ion-to-neutral ratios within the layer will be examined.

Results will be interpreted in terms of the general reaction schemes which have recently emerged (for example Swider, 1969; Narcisi, 1968 and Ferguson and Fehsenfeld, 1968).

A brief discussion of the theory of resonance fluorescence will be presented first, to establish the physical process used in the measurement. Because of its inherent simplicity it provides a means of highly accurate density measurements in an absolute sense for both the ionized and neutral species commonly associated with sporadic E events.

The Experiment

A Nike-Apache sounding rocket was launched from Wallops Island, Virginia, on June 28, 1969, at 00.35 GMT (evening twilight), with a solar depression angle of 1.44°. On board was a 250 mm focal length Ebert-Fastie scanning spectrometer with a spectral resolution of 5 Å encompassing the spectral region from 2750 to 3225 Å. The instrument's optical axis was aligned approximately in the zenith direction throughout the flight until the rocket turned over at 78 km on the downward leg. Apogee was 106 km with a total horizontal range of 86 km and a launch azimuth of 120°.

Figure 1 shows the optical and mechanical layout of the instrument which may conveniently be viewed in three parts: (1) a detector head which houses the photomultiplier tube, electrometer and high voltage supply for the phototube; (2) the spectrometer chamber with associated optics and (3) a bulkhead section that houses the 28 volt internal power source and all elec-

tronics exclusive of the electrometer. For a detailed description of the optical characteristics of the spectrometer see Fastie (1952).

Absolute calibration of the detector head was accomplished using a tungsten source at a known temperature, using an NBS calibrated pyrometer accurate to ± 10 °K. A pass band filter calibrated at the National Center for Atmospheric Research to a precision of ± 3% was used to isolate the wavelength of the absolute calibration at 2972 Å.

The relative response of the photomultiplier over the spectral interval used in the experiment was determined using sodium salicylate. This introduces an error of ± 4% between the wavelength of the Mg^+ doublet at 2800 Å and the wavelength of the absolute calibration at 2972 Å.

To determine the transmission of the optics as a function of wavelength a double monochromator was used to isolate emission lines from a hollow cathode

cadmium source in order to normalize the transmission measurements. The optical system was calibrated in the flight configuration to eliminate inconsistencies resulting from alterations in the geometry between the laboratory and actual flight conditions. This phase of the calibration was accurate to ± 2%.

With proper accounting for uncertainties in the geometry of the absolute calibration and for non-linearities in the voltage measuring devices, the precision of the entire instrumental calibration is ± 30 percent.

Theory of Resonance Fluorescence

Singly ionized magnesium has two allowed transitions in the near ultraviolet which form a closely spaced doublet at 2802.698 Å corresponding to the $3s\ ^2S_{\frac{1}{2}}$ - $3p\ ^2P_{\frac{1}{2}}$ transition and 2795.523 Å corresponding to the $3s\ ^2S_{\frac{1}{2}}$ - $3p\ ^2P_{\frac{3}{2}}$ transition. Quantities referring to these two transitions will be subscripted by a (1/2, 1/2) in the case of 2802 Å and (1/2, 3/2) in the case of 2795Å. Neutral magnesium has a single allowed transition at 2852.13 Å corresponding to the $3s^2\ ^1S_0$ - $3s3p\ ^1P_1$ transition, which we will designate by a (0,1) subscript on the relevant quantities.

Chamberlain (1961) discusses resonance scattering and fluorescence in terms of an "emission rate factor", g which is the proportionality factor between the apparent column emission rate and the column density in the case of single scattering. Physically, g is the product of the source intensity (in this case the solar flux) and

the effective scattering cross section. The brightness of a diffuse airglow source $4\pi\mathcal{I}$ in photons $cm^{-2}sec^{-1}$ $column^{-1}$ may, for the 3s $^2S_{\frac{1}{2}}$ - 3p $^2P_{\frac{1}{2}}$ case for example, be written

$$4\pi\mathcal{I}_{\frac{1}{2},\frac{1}{2}} = g_{\frac{1}{2},\frac{1}{2}}\ \eta/\mu = \pi\mathcal{J}_{\frac{1}{2},\frac{1}{2}}\ \sigma_{\frac{1}{2},\frac{1}{2}}\ \eta/\mu$$

$$= \pi\mathcal{J}_{\frac{1}{2},\frac{1}{2}}\ \frac{\pi e^2}{mc^2}\ f_{\frac{1}{2},\frac{1}{2}}\ \eta/\mu$$

where

η is the column density of ionized magnesium in cm^{-2}

μ is the slant path correction, $\cos\theta$

$\pi\mathcal{J}_{\frac{1}{2},\frac{1}{2}}$ is the solar flux in photons $cm^{-2}sec^{-1}$ $\mathring{A}^{-1}$ at the wavelength of the $^2S_{\frac{1}{2}}$ - $^2P_{\frac{1}{2}}$ transition

$\sigma_{\frac{1}{2},\frac{1}{2}}$ is the effective scattering cross section

$f_{\frac{1}{2},\frac{1}{2}}$ is the oscillator strength of the transition

e,m have their conventional meaning as the charge and mass of the electron.

The oscillator strength of each transition considered here is listed in Allen (1955), (section #28). Citing those values:

$f_{\frac{1}{2},\frac{1}{2}} = .3$	(Mg^+, 2802.698 Å)
$f_{\frac{1}{2},\frac{3}{2}} = .6$	(Mg^+, 2795.523 Å)
$f_{0,1} = 1.6$	(Mg, 2852.13 Å)

Therefore, in order to relate column density to column emission rate, it remains only to determine the solar flux at the wavelength of each transition. For the ionized doublet the problem is complicated to some degree by the existence of significant amounts of Mg^+ in the solar atmosphere as evidenced by a sample of the solar spectrum (Purcell et al., 1962) shown in Figure 2. Fortunately, because of its importance in solar line formation, the magnesium doublet has received extensive study at high resolution (for example: Purcell et al., 1962; Lemaire and Blamont, 1967; Lemaire, 1970; Bates et al., 1970). A profile published by Lemaire (1970)

with a resolution of 35 mm Å is shown in Figure 3. In order to determine the solar flux at the center of the reversal, the integrated number of photons cm^{-2} sec^{-1} (Wilson et al., 1954) over each line was used to normalize the Lemaire profile to absolute units, resulting in

$$\pi \mathcal{I}_{\frac{1}{2},\frac{1}{2}} = 1.78 \times 10^{12} \text{ photons } cm^{-2} sec^{-1} \text{ Å}^{-1}$$

$$\pi \mathcal{I}_{\frac{1}{2},\frac{3}{2}} = 2.21 \times 10^{12} \text{ photons } cm^{-2} sec^{-1} \text{ Å}^{-1}$$

Neutral magnesium is far less prevalent in the solar atmosphere and thus the 100 m Å data of Wilson et al. (1954) was used directly, resulting in

$$\pi \mathcal{I}_{1,0} = 4.91 \times 10^{11} \text{ photons } cm^{-2} sec^{-1} \text{ Å}^{-1}$$

Appropriate values for the emission rate factors are therefore:

$$g_{\frac{1}{2},\frac{1}{2}} = \pi \mathcal{I}_{\frac{1}{2},\frac{1}{2}} \frac{\pi e^2}{mc^2} \lambda^2_{\frac{1}{2},\frac{1}{3}} f_{\frac{1}{2},\frac{1}{2}} = .037 \text{ photons/sec}$$

$$g_{\frac{1}{2},\frac{3}{2}} = \pi \mathcal{I}_{\frac{1}{2},\frac{3}{2}} \frac{\pi e^2}{mc^2} \lambda^2_{\frac{1}{2},\frac{3}{2}} f_{\frac{1}{2},\frac{3}{2}} = .091 \text{ photons/sec}$$

and

$$g_{o,1} = \pi \mathcal{J}_{o,1} \frac{\pi e^2}{mc^2} \lambda_{o,1}^2 f_{o,1} = .056 \text{ photons/sec}$$

In the section that follows, these emission rate factors will be used to relate the experimentally determined column emission rate to the appropriate column density.

Experimental Results

A number of interesting observations concerning the morphology of the ionized layer were noticed. From the commencement of data acquisition at 56 kilometers to an altitude of 87 kilometers, corresponding to a time span of 39 seconds and a horizontal displacement of 12.3 kilometers, no detectable Mg^+ signal was noticed. During this period the instrument was passing through the region of intense Rayleigh scattering, the study of which constituted the primary experiment in a search for ultraviolet emission from the hydroxyl radical. An example of a data frame at 87 kilometers is shown in Figure 4. This is a typical spectrum during this period of the experiment and an examination of the region around 2800 Å reveals no perceptable signal other than the Rayleigh scattered background. On the very next data frame (Figure 5) however, a clear spectrum of the Mg^+ doublet began to appear. The period between scans, 2.6 seconds, corresponds to a horizontal displacement of .8 km.

To facilitate a description of the spatial characteristics of the cloud, Figure 6 shows the time development of the signal strength as a function of time and of the instrument's horizontal displacement. It is apparent that the ionized cloud has a clearly defined edge with a rather constant column density along the interior of the cloud. Some structure is present, however, over the 42 horizontal kilometers surveyed by the instrument until the vehicle turned over on the downleg. A typical spectrum taken under the cloud is shown in Figure 7.

As mentioned previously, the rocket attained an altitude of 106 km but did not pass through the cloud and apparently did not significantly penetrate the region of Mg^+ emission because the signal did not appreciably decrease near apogee (see Figure 6).

An ionogram taken just as the rocket reached 80 km on the upleg is shown in Figure 8. Data taken for this ionogram were reduced by W. R. Wright of the ESSA Laboratories in Boulder. The altitude of peak ionization was found to be 108.6 km ± 2 km with a blanketing

frequency of 2.2 MC, corresponding to an electron density within the sporadic E layer of $6 \times 10^4 cm^{-3}$ (see Reddy and Rao, 1968).

In order to make a rough estimate of the peak volume density of Mg^+ in the layer the emission rate factor for 1/2 - 3/2 transition (calculated in the previous section) was divided into a representative column emission rate of 400 Rayleighs to yield a column density of $4 \times 10^9 cm^{-2}$. A model for the layer was then assumed, guided by the mass spectrometer data of Narcisi (1968). The layer model is shown in Figure 9 and is characterized by a principal layer of half width equal to 2 km and wings extending 5 km into the background ionization, one order of magnitude below the level of peak ionization. Using a column density of $4 \times 10^9 cm^{-2}$ and this layer model, a peak ion density of $2 \times 10^4 cm^{-3}$ was deduced. This then corresponds to approximately 30 percent of the peak ionization within the layer.

In order to determine the ratio of ionized to neutral magnesium, all of the spectral scans were added together. The results are shown in Figure 10. It is clear from examining the summed data that no obvious signal is present resulting from neutral magnesium at 2852 Å. Assuming an upper limit of 10 Rayleighs for the Mg signal, the ion neutral ratio is found to be

$$\frac{Mg^+}{Mg} \geq \left(\frac{360 \text{ Rayleighs}}{10 \text{ Rayleighs}}\right)\left(\frac{.056}{.091}\right) = 22.2$$

which represents the ratio of the signal intensity scaled by the appropriate ratio of the emission rate factors. The next section investigates the photochemical implications of this ratio.

Interpretation of Results

The photochemistry of layered metallic ions has ben extensively considered; first with regard to sodium (Blamont and Donahue, 1964; Hunten, 1967) and later for the E region species, silicon, magnesium and iron (Axford and Cunnold, 1966; Donahue, 1966; Whitehead, 1966; Gleeson, 1967; Ferguson and Fehsenfeld, 1968; Narcisi, 1968; Swider, 1969). Although temperate latitude sporadic E events appear to be highly complicated and rather variable in character, a somewhat simplified equilibrium model will be adopted to investigate the implications of the data on the ion-neutral ratio presented in the previous section. Attention will be directed primarily toward a determination of the charge transfer rates between Mg and the ionized species NO^+ and O_2^+. Figure 11 represents a schematic of the reactions listed in Table I which constitute the twelve processes thought to be of primary importance (see Ferguson and Fehsenfeld, 1968; Narcisi, 1968; Swider, 1969).

Although the layering of metallic species is inherently a time-dependent problem (see Gleeson, 1967), diffusion will not be considered. Rather, an attempt will be made to draw conclusions concerning the rapid exchange reactions, which have characteristic times significantly less than the lifetime of the sporadic E layer. Presumably, the ultimate sink for the Mg atoms is downward diffusion and the ultimate source is meteor ablation. Times for removal by diffusion will also be taken as significantly larger than the time required for the Mg^+/Mg ratio to be determined by chemical equilibrium, that is, the question whether magnesium enters the reaction scheme as Mg^+ or as Mg from meteor deposition is not considered.

Lifetimes for each of the reactions are indicated in Figure 11 by the number immediately above the arrow indicating the direction of the reaction. The altitude of the layer is assumed to be approximately 110 km with a local ozone density of 10^4 cm^{-3} and an atomic oxygen density of 10^{11} cm^{-3}. The electron density is taken as 6×10^4 cm^{-3}; the N_2 and O_2 densities are 1.6×10^{12} cm^{-3} and 3.5×10^{11} cm^{-3} respectively (U. S. Standard Atmos-

pheres, 1966). Table I lists the relevant reactions and associated reaction rates. Examination of the characteristic times shown in Figure 11 serves to demonstrate four points:

(1) The lifetimes of MgO_2^+, MgO^+, and Mg are shorter than one hour (in the case of MgO_2^+ and MgO^+, shorter than one second).

(2) Mg^+ has a lifetime dictated by the three-body reaction with N_2 and O_2, which is on the order of a day, allowing Mg^+ to form an ionization layer (Gleeson, 1967).

(3) Destruction rates of MgO_2^+ and MgO^+ are determined by the oxidation reactions involving atomic oxygen and not by dissociative recombination.

(4) Neutral magnesium is destroyed primarily by charge exchange with NO^+ and O_2^+. Possible products of this charge exchange include Mg^+ and MgO^+, with Mg^+ production being five times as efficient as MgO^+ (Ferguson and Fehsenfeld, 1968) for the case of O_2^+. The NO^+ charge transfer rate is assumed to be similar.

Guided by the above analysis, four chemical equilibrium reactions for MgO_2^+, MgO^+, Mg^+ and Mg may be written as follows:

$$(1) \qquad [MgO_2^+] = \frac{k_1 [O_2]\ [N_2]\ [Mg^+]}{k_3\ [O]}$$

$$(2) \qquad [MgO^+] = \frac{k_2\ [Mg^+]\ [O_3] + k_3\ [MgO_2^+]\ [O] + [Mg]\ \left\{k_4 [O_2^+] + k_5\ [NO^+]\right\}}{k_6 [O]}$$

$$(3) \qquad [Mg^+] = \frac{k_6 [MgO^+]\ [O] + k_7\ [O_2^+]\ [Mg] + k_8\ [NO^+]\ [Mg] + J_9\ [Mg]}{k_1\ [O_2]\ [N_2]}$$

$$(4) \qquad [Mg] = \frac{k_{10} [Mg^+]\ [e] + \alpha_{11}\ [MgO^+]\ [e] + \alpha_{12}\ [MgO_2^+]\ [e]}{\left(k_4 + k_7\right)\ [O_2^+] + \left(k_5 + k_8\right)\ [NO^+] + J_9}$$

TABLE I

Reaction	Reaction Rate	Reference
$Mg^+ + O_2 + M \rightarrow MgO_2^+ + M$	$k_1 = 2.5 \times 10^{-10}$ cm^6 sec^{-1}	(Ferguson & Fehsenfeld, 1968)
$Mg^+ + O_3 \rightarrow MgO^+ + O_2$	$k_2 = 2.3 \times 10^{-11}$ cm^3 sec^{-1}	(Ferguson & Fehsenfeld, 1968)
$MgO_2^+ + O \rightarrow MgO^+ + O_2$	$k_3 = 1 \times 10^{-10}$ cm^3 sec^{-1}	(Estimate; Swider, 1969)
$Mg + O_2^+ \rightarrow MgO^+ + O$	$k_4 < 5 \times 10^{-10}$ cm^3 sec^{-1}	see text
$Mg + NO^+ \rightarrow MgO^+ + N$	$k_5 < 5 \times 10^{-10}$ cm^3 sec^{-1}	see text
$MgO^+ + O \rightarrow Mg^+ + O_2$	$k_6 = 1 \times 10^{-10}$ cm^3 sec^{-1}	(Ferguson & Fehsenfeld, 1968)
$Mg + O_2^+ \rightarrow Mg^+ + O_2$	$k_7 = ?$	
$Mg + NO^+ \rightarrow Mg^+ + NO$	$k_8 = ?$	
$Mg + h\nu \rightarrow Mg^+ + e$	$j_9 = 4 \times 10^{-7}$ sec^{-1}	(Swider, 1969)
$Mg^+ + e \rightarrow Mg + h\nu$	$r_{10} = 1 \times 10^{-12}$ cm^3 sec^{-1}	(Estimate from Bates and Dalgarno, 1962)
$MgO^+ + e \rightarrow Mg + O$	$\alpha_{11} \approx 1 \times 10^{-7}$ cm^3 sec^{-1}	(Estimate; Swider, 1969)
$MgO_2^+ + e \rightarrow Mg + O_2$	$\alpha_{12} = 3 \times 10^{-7}$ cm^3 sec^{-1}	(Estimate; Swider, 1969)

To simplify the equilibrium equation for $[MgO^+]$ consider the following: Equation (1) allows the ratio between $[MgO_2^+]$ and $[Mg^+]$ to be calculated in terms of the atmospheric constituents at 110 km:

$$\frac{[MgO_2^+]}{[Mg^+]} = 1.4 \times 10^{-7} \tag{5}$$

Examination of the numerator of Equation (2) with this ratio in mind reveals that the reaction of MgO_2^+ with O is ten times as effective in producing MgO^+ as the reaction of Mg^+ with O_3.

Equation (2) may be further simplified: guided by Narcisi's (1968) discussion of $[O_2^+]$ and $[NO^+]$ response to the layering of metallic ions, the following somewhat arbitrary choices for the reduction in NO^+ and O_2^+ densities at the peak of the layer are adopted:

$[NO^+]$	$= 5.3 \times 10^4$ cm^{-3}	without metallic layering (Norton and Barth, 1970)
$[NO^+]^1$	$= 1.6 \times 10^4$ cm^{-3}	at metal ion peak
$[O_2^+]$	$= 5 \times 10^4$ cm^{-3}	without metal layering (Norton and Barth, 1970)
$[O_2^+]^1$	$= 2.5 \times 10^4$ cm^{-3}	at metal ion peak

The more efficient charge transfer from NO^+ to Mg to form Mg^+ than from O_2^+ to Mg to form Mg^+ is a result cited by Narcisi (1968) who found $k_8/k_7 \simeq 10$.

If the assumption is made that the charge transfer rate coefficients k_4 and k_5 are 10^{-10} or smaller, equation (2) becomes:

$$[MgO^+] = \frac{k_3\ [O]\ [MgO_2^+]}{k_6\,[O]} \tag{6}$$

This choice of an upper limit for k_4 and k_5 will be justified in the final result. Reference to Table I indicates that $k_3 = k_6$, so Equation (6) reduces to

$$[MgO^+] = [MgO_2^+]$$

The numerator of Equation (4) may be simplified, however, because

$$\frac{\alpha_{12}\,[MgO_2^+]\,[e]}{r_{10}\,[Mg^+]\,[e]} \simeq 10^{-2} \qquad \text{using equation (5)}$$

and

$$\alpha_{11}\,[MgO_2^+]\,[e] \simeq \alpha_{12}\,[MgO^+]\,[e] \text{ from equation (6)}$$

Assuming that the charge transfer reactions dominate the photoionization reaction, we have the result that

$$[Mg^+]/[Mg] \simeq \frac{k_7\ [O_2^+] + k_8\ [NO^+]}{r_{10}[e]}$$

From the ratio determined in the experiment

$[Mg^+]/[Mg] \geq 22$

it may be determined that

$$k_7 \geq 7.3 \times 10^{-12} \text{ and } k_8 \geq 7.3 \times 10^{-11}$$

Although the chemistry to this point has adopted the suggested rate of 1×10^{-10} cm^3/sec (Swider 1969) for the reaction between MgO_2^+ and atomic oxygen, it should be emphasized that this result is without experimental verification. In fact, the reaction may be inoperative which would be accounted for in the reaction scheme as follows:

Equation (1) would be replaced by

$$(MgO_2^+) = \frac{k_1 [O_2] [N_2] [Mg^+]}{\alpha_{12}[e]} \tag{7}$$

resulting in an MgO_2^+ to Mg^+ ratio of 7.7×10^{-5}; or an increase of more than two orders of magnitude in the MgO_2^+ concentration.

Equation (4) then becomes

$$(Mg) = \frac{\alpha_{12}[MgO_2^+] [e]}{k_7[O_2^+] + k_8[NO^+]} \tag{8}$$

Combining (7) and (8) results in an expression for the ion-neutral ratio

$$[Mg^+]/[Mg] = \frac{k_7 [O_2^+] + k_8 [NO^+]}{k_1 [O_2] [N_2]} \geq 22$$

in turn implying that

$$k_7 \geq 1.5 \times 10^{-10} \text{ cm}^3 \text{ sec}^{-1}$$

$$k_8 \geq 1.5 \times 10^{-9} \text{ cm}^3 \text{ sec}^{-1}$$

This indicates that a greater burden is placed upon the charge exchange reactions if the $MgO_2^+ + O \rightarrow MgO^+ + O_2$ path is closed. Examination of the reaction schematic serves to clarify this because the principal removal process for Mg^+ ($Mg^+ + O_2 + N_2 \rightarrow MgO_2 + N_2$) results in a direct increase in Mg production instead of a simple recycling process through MgO^+.

Discussion

Starting with the information that the charge transfer reaction of Mg with NO^+ is a dominant one in the production of Mg^+ (based on Narcisi's ion mass spectrometer measurements) we deduced that rate of this reaction must be greater than 7×10^{-11} cm^3 sec^{-1} if the radiative recombination rate is 1×10^{-12} cm^3 sec^{-1}, and the reaction rate of $MgO_2^+ + O \rightarrow MgO^+ + O$ is 10^{-10} cm^3/sec. On the other hand, if the reaction between atomic oxygen and MgO_2^+ is inoperative, the charge exchange rate must be $\geq 1.5 \times 10^{-9}$ cm^3/sec. Without the ion mass spectrometer information, we could have, as well, deduced that the equilibrium between Mg and Mg^+ is determined by photoionization of Mg and radiative recombination of Mg^+, resulting in the latter rate being less than 3×10^{-13} cm^3 sec^{-1}. If the rate of this Mg charge exchange reaction with NO^+ or O_2^+ to produce MgO^+ is actually as large as 5×10^{-10} cm^3 sec^{-1}, then the MgO^+ density will begin to play an important role in determining the Mg - Mg^+ ratio and the approximation leading to equation (6) breaks down.

Summary

Dayglow observations of the 2795, 2803 Å doublet of MgII and an upper limit on the 2852 Å line of MgI show that the density at Mg^+ is greater than that of Mg in a sporadic E region. These observations are consistent with a theory where the magnesium atoms and ions are put into the atmosphere by ablation of micrometeorites, and the equilibrium between the Mg and Mg^+ is determined by charge-transfer from NO^+ to Mg to produce Mg^+ and by radiative recombination of Mg^+ with electrons to reform Mg. If the radiative recombination rate is 10^{-12} cm^3 sec^{-1} then the charge transfer rate is greater than 7×10^{-11} cm^3 sec^{-1}. Since the scanning spectrometer experiment that made the dayglow measurements was not specifically designed to study MgI and MgII, the experiment was not optimized for these measurements. Such an optimum experiment using either photometers or a spectrometer, should be able to determine the actual ion-neutral ratio simultaneously for Mg, Fe and Si as a function of altitude within the layer if the rocket penetrates the sporadic E layer.

REFERENCES

Allen, C. W., "Spectra: Permitted Atomic Oscillator Strengths," in Astrophysical Quantities, The Athlone Press, London, 1963.

Axford, W. I., and D. M. Cunnold, "The Wind-Shears Theory of Temperate Zone Sporadic E," Radio Science, 1, 191, 1966.

Bates, D. R., and A. Dalgarno, "Electronic Recombination," in Atomic and Molecular Processes, edited by D. R. Bates, Academic Press, New York, 1962.

Bates, B., D. J. Bradley, C. D. McKeith, N. E. McKeith, W. M. Burton, H. J. B. Paxton, D. V. Shenton and R. Wilson, "Fabry-Perot Interferograms of the Solar MgII Resonance Lines," in Ultraviolet Stellar Spectra and Related Ground-Based Observations, edited by L. Houziaux and H. E. Butler, D. Reidel Publishing Co., 1970.

Blamont, J. E., and T. M. Donahue, "Sodium Dayglow: Observations and Interpretation of a Large Diurnal Variation," J. Geophys. Res., 69, 4093, 1964.

Chamberlain, J. W., "Theory of the Twilight and Day Airglow: Resonance Scattering and Fluorescence for an Optically Thin Layer," in Physics of the Aurora and Airglow, Academic Press, New York, 1961.

Donahue, T. M., "On the Ionospheric Conditions in the D-Region and Lower E Region." J. Geophys. Res., 71, 2237, 1966.

Fastie, W. G., "A Small Plane Grating Monochromator," J. Opt. Soc. Am., 42, 641, 1952.

Fehsenfeld, F. C., A. L. Schmeltekopf, P. D. Goldan, H. I. Schiff, and E. E. Ferguson, "Thermal Energy Ion-neutral reaction Rates, 1, Some reactions of Helium Ions," J. Chem. Phys. 44, 4087, 1966.

Fehsenfeld, F. C., E. E. Ferguson, and A. L. Schmeltekopf, "Metal Ion Reactions with Ozone," Bull. Am. Phys. Soc., 13, 212, 1968.

Ferguson, E. E., F. C. Fehsenfeld, P. D. Goldan, and A. L. Schmeltekopf, "Positive ion-neutral Reactions in the Ionosphere," J. Geophys. Res., 70, 4323, 1965.

Ferguson, E. E., and F. C. Fehsenfeld, "Some Aspects of the Metal Ion Chemistry of the Earth's Atmosphere," J. Geophys. Res., 73, 6215, 1968.

Gleeson, L. J., "Positive ion layers in the E-region of the Ionosphere," Planet. Space Sci., 15, 27, 1967.

Hunten, D. M., "Spectroscopic Studies of the Twilight Airglow," Space Sci. Rev. 6, 493, 1967.

Istomin, V. G., "Ions of Extra-terrestrial Origin in the Earth's Ionosphere," Space Research III, North-Holland, Amsterdam, 1963.

Lemaire, P., and J. E. Blamont, "Stigmatic Balloon Spectra of the Solar Mg II Doublet," Astrophys. Letters, 150, L129, 1967.

Lemaire, P., "Resonance Lines in the Solar Chromosphere," in Ultraviolet Stellar Spectra and Related Ground-Based Observations, edited by L. Houziaux and H. E. Butler, D. Reidel Publishing Co., 1970.

McKinley, D. W. R., "Radio Technique," in Meteor Science and Engineering, McGraw-Hill Publishing Co., New York, 1961.

Narcisi, R. S., A. D. Bailey and L. Della Lucca, "Composition Measurements of Sporadic E in the Nightime Lower Ionosphere," in Space Research VII, 123, North-Holland, Amsterdam, 1967.

Narcisi, R. S., "Processes Associated with Metal-ion Layers in the E-Region of the Ionosphere," in Space Research VIII, 360, North-Holland, Amsterdam, 1968.

Norton, R. B., and C. A. Barth, "Theory of Nitric Oxide in the Earth's Atmosphere," J. Geophys. Res., 75, 3903, 1970.

Purcell, J. D., Garrett, D. L., and R. Tousey, "Solar Spectra from 3500 to 2200 Å at 30 mÅ Resolution," in Space Research III, North-Holland, Amsterdam, 1962.

Reddy, C. A., and M. Mukunda Rao, "On the Physical Significance of the Es Parameters fbEs, fEs, and foEs," J. J. Geophys. Res., 73, 215, 1968.

Rosenberg, N. W., "Chemical Releases at High Altitudes," Science 152, 1017, 1966.

Swider, W., Jr., "Processes for Meteroic Elements in the E-Region," Planet. Space Sci., 17, 1233, 1969.

U. S. Standard Atmosphere Supplements, 1966, U. S. Government Printing Office, Washington, D. C. 20402.

Whitehead, J. D., "Mixtures of Ions in the Wind-Shear Theory of Sporadic E," Radio Science 1, 196, 1966.

Wilson, N., R. Tousey, J. D. Purcell, F. S. Johnson, and C. E. Moore, "A Revised Analysis of the Solar Spectrum from 2900 Å to 2635 Å," Astrophys. J., 119, 590, 1954.

LIST OF FIGURES

LIST OF FIGURES

INSTRUMENTAL SCHEMATIC

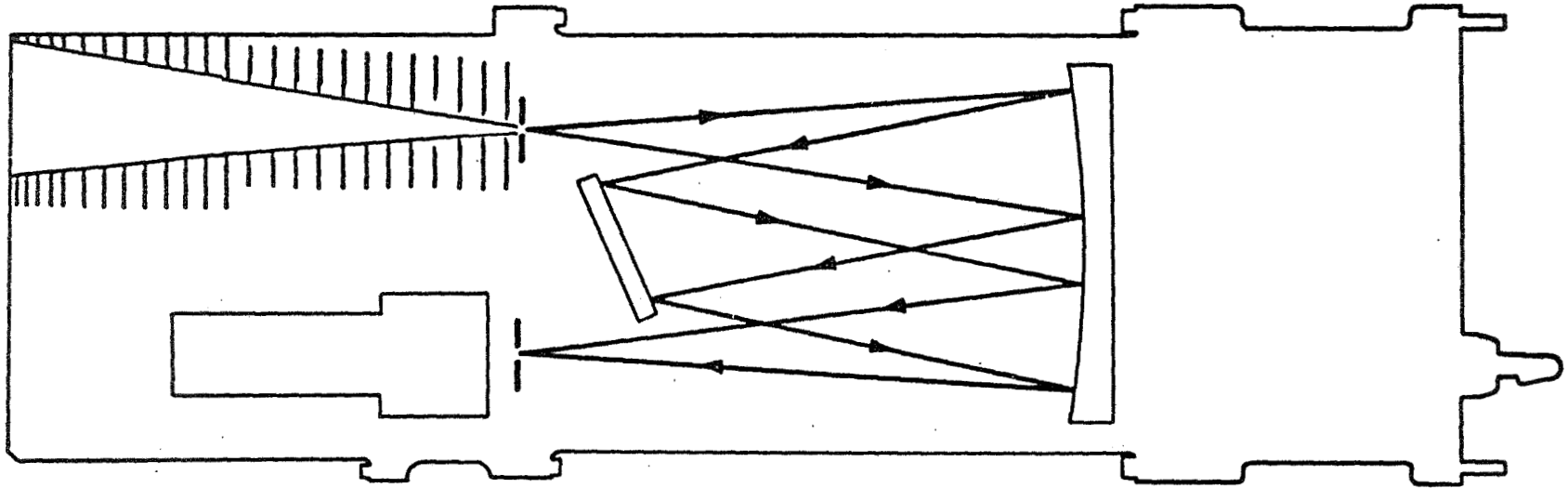

Figure 1 Optical and Mechanical Schematic of the Instrument.

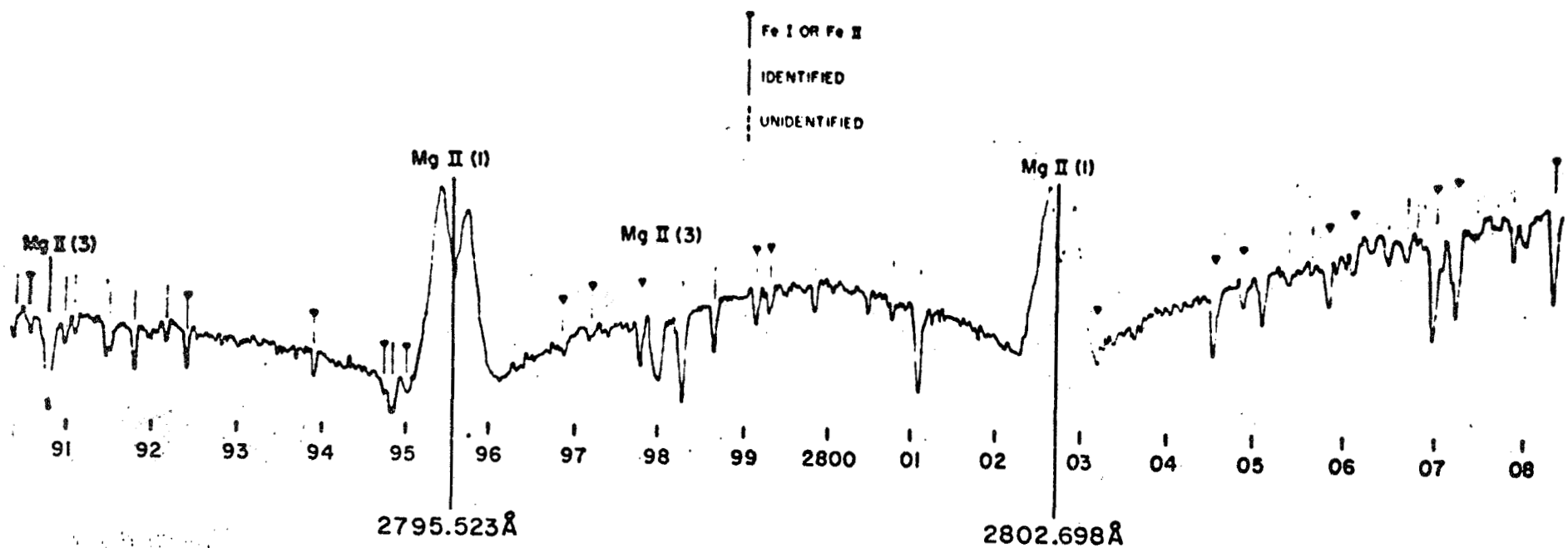

Figure 2 Solar Spectrum (Purcell et al., 1962)

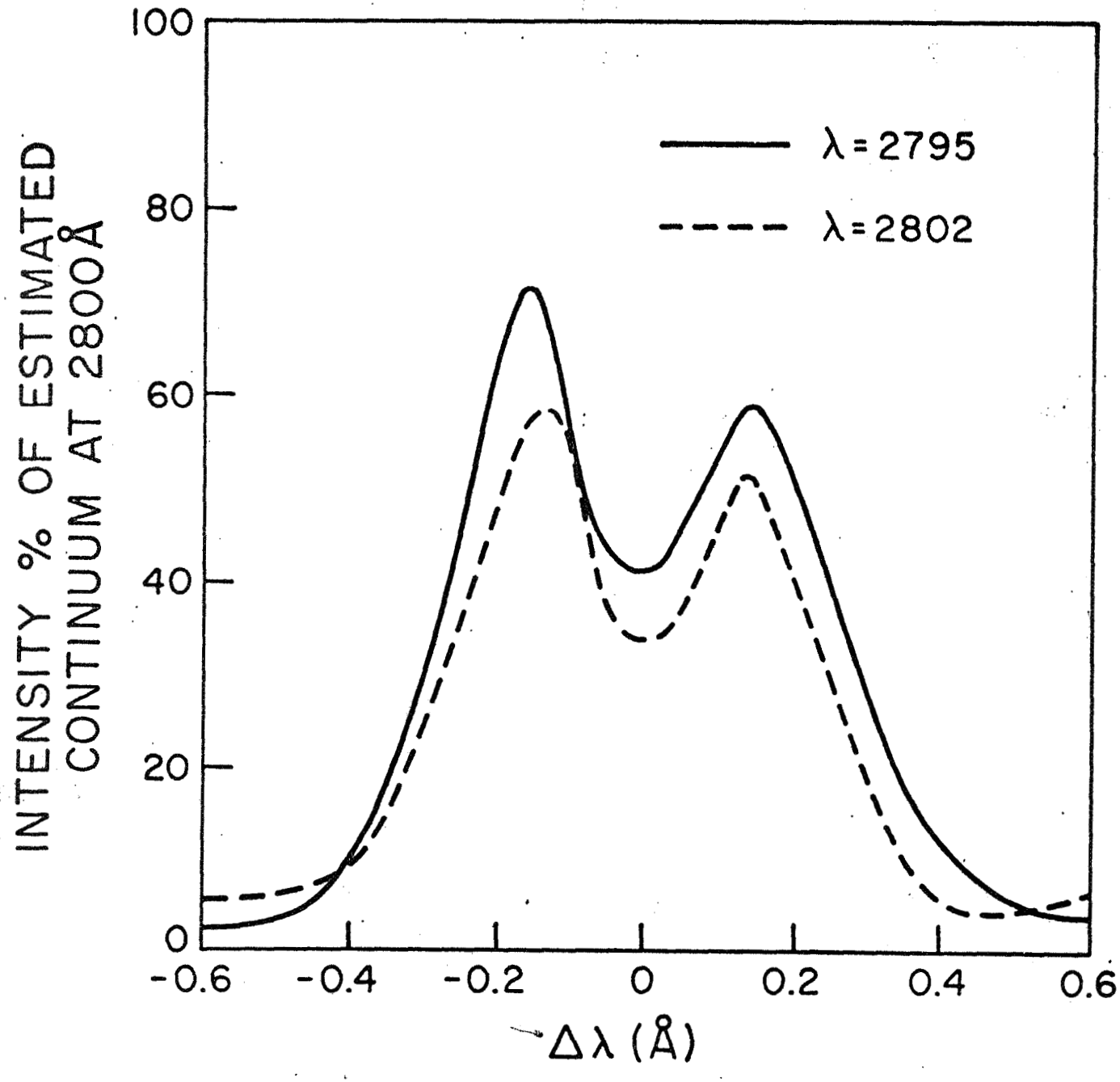

Figure 3 High Resolution Profile of the MgII Doublet.

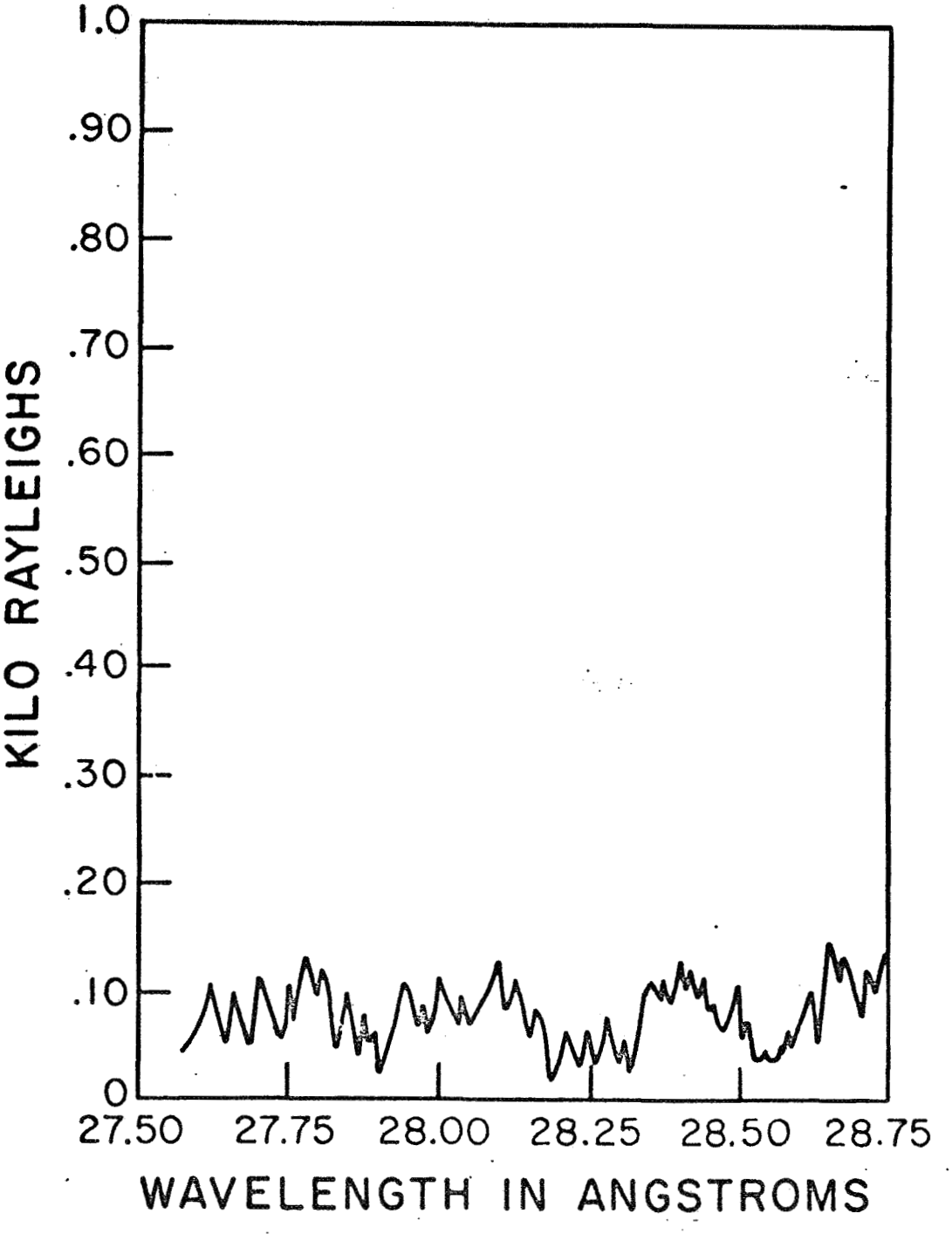

Figure 4 Data Frame at 87 Kilometers Showing No Recognizable Signal from Mg^{+}.

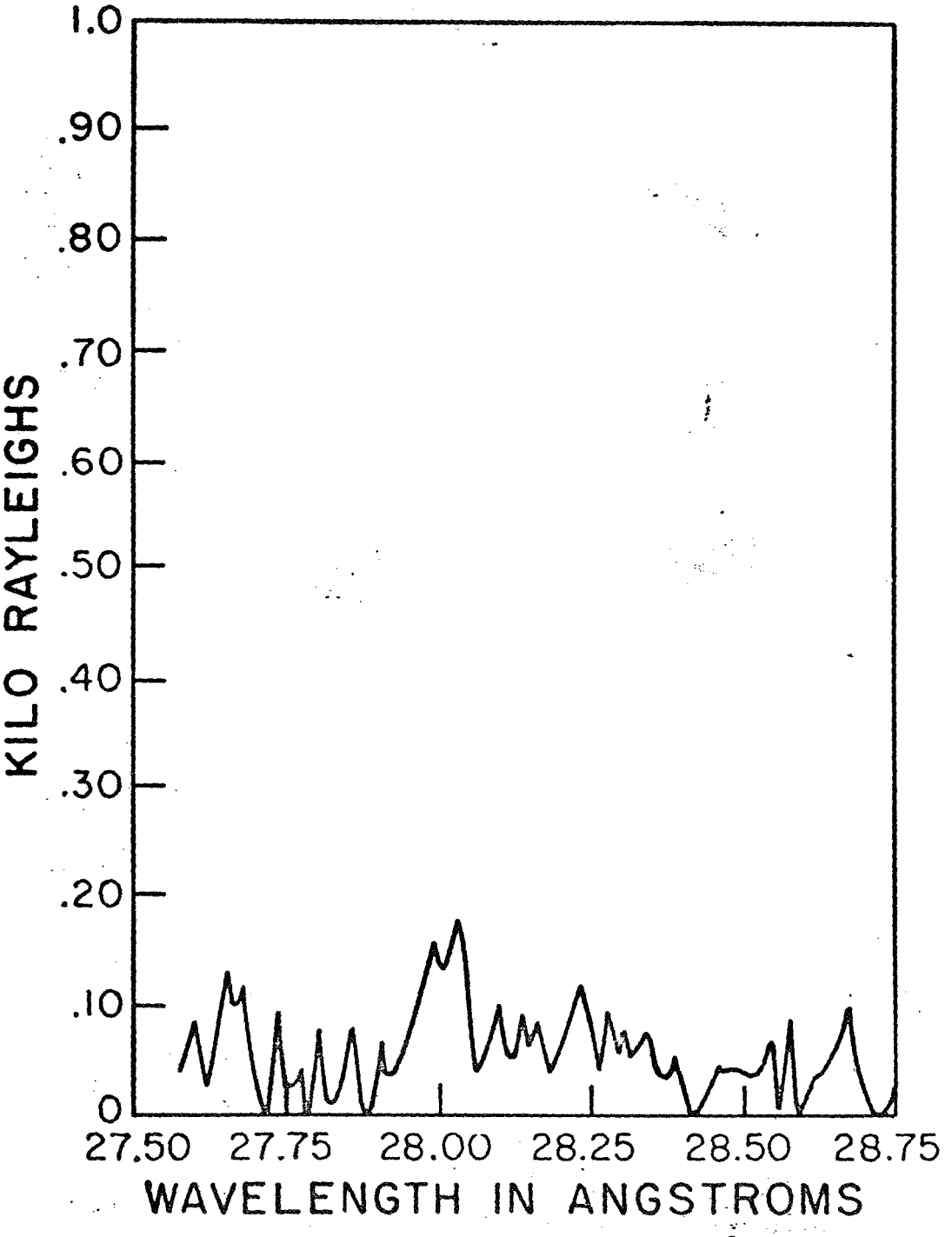

Figure 5 First Data Frame with Measurable Mg^{+} Signal.

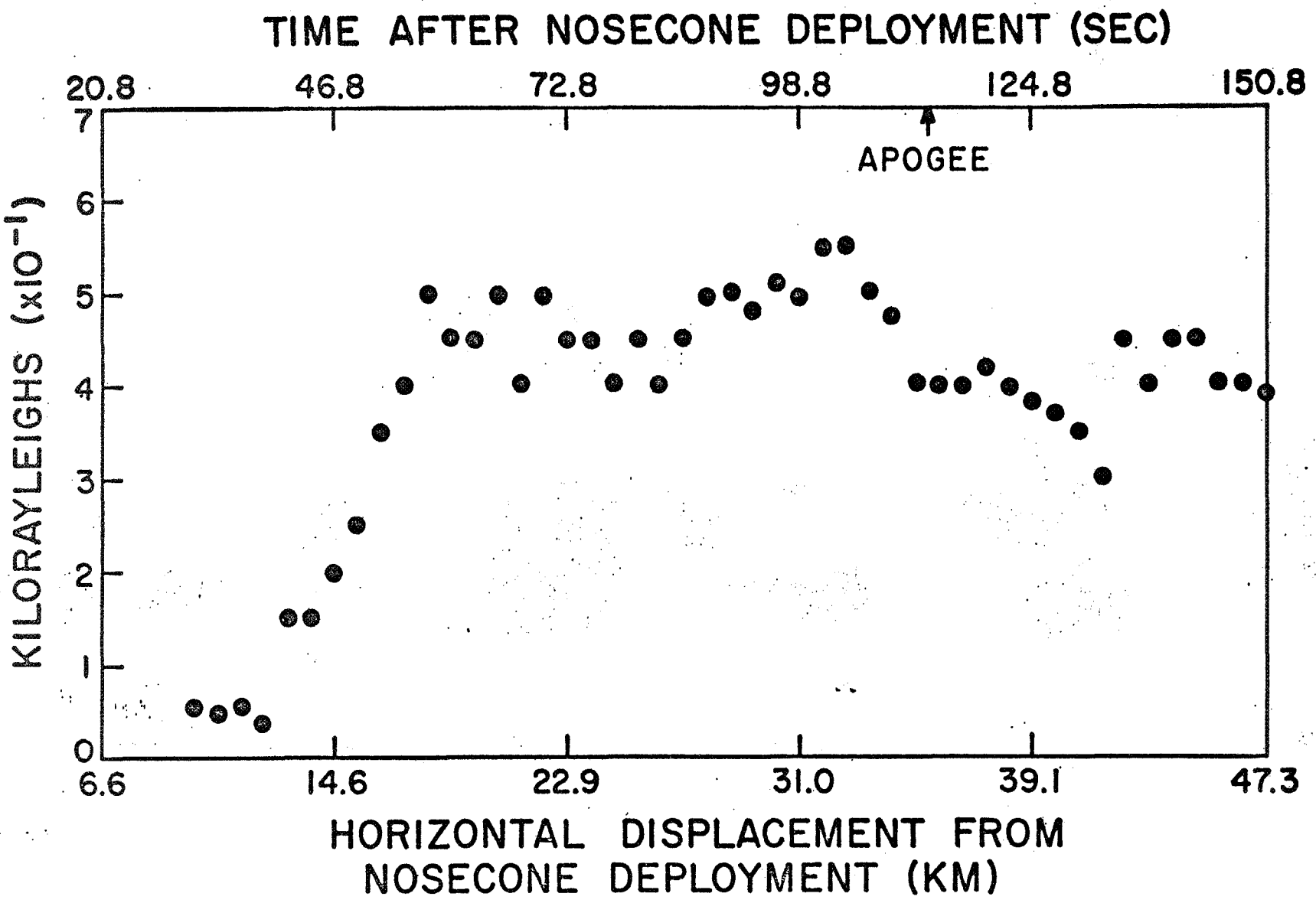

Figure 6 Time Development of Signal.

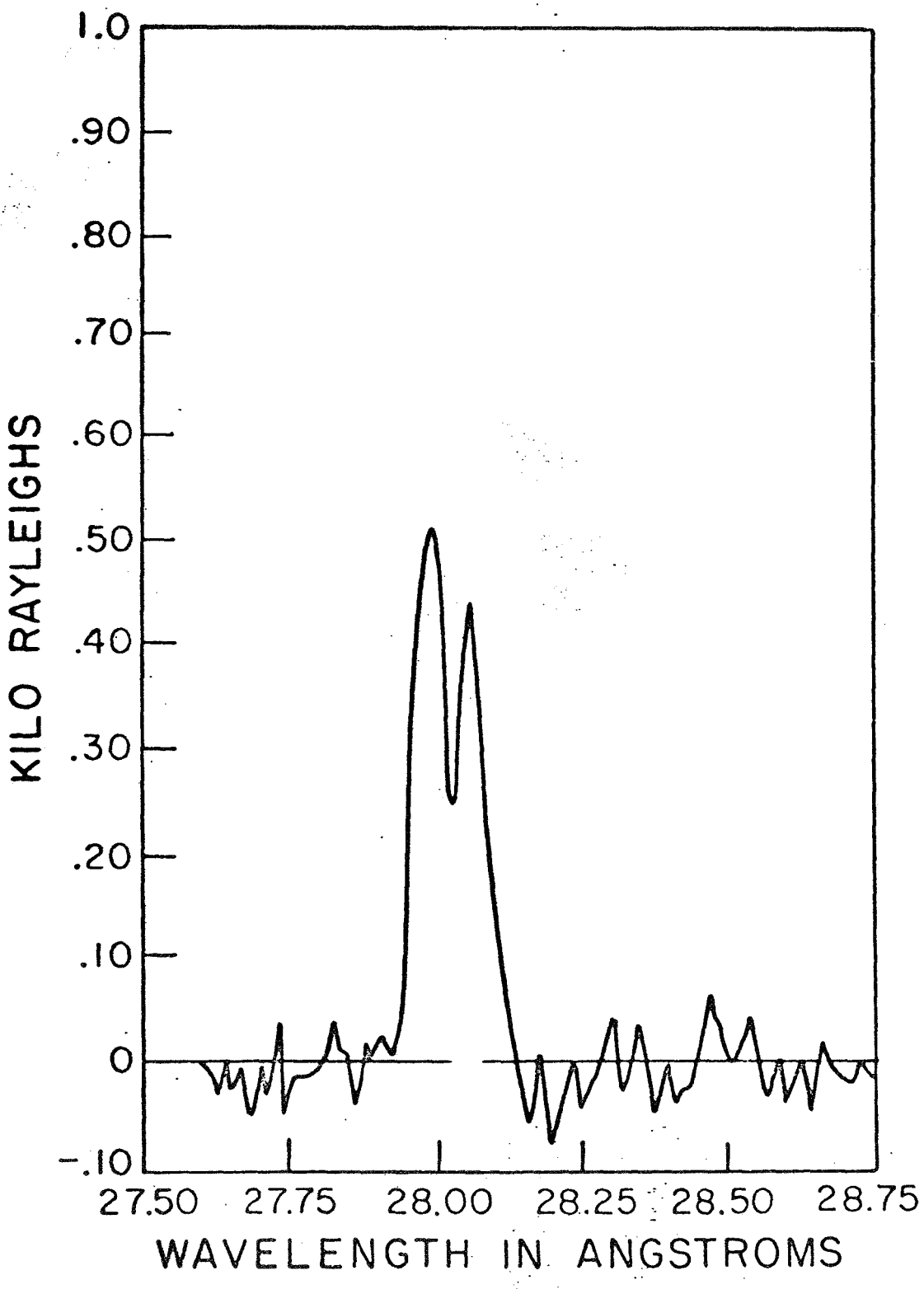

Figure 7 Typical Spectrum of the MgII Doublet within the Cloud.

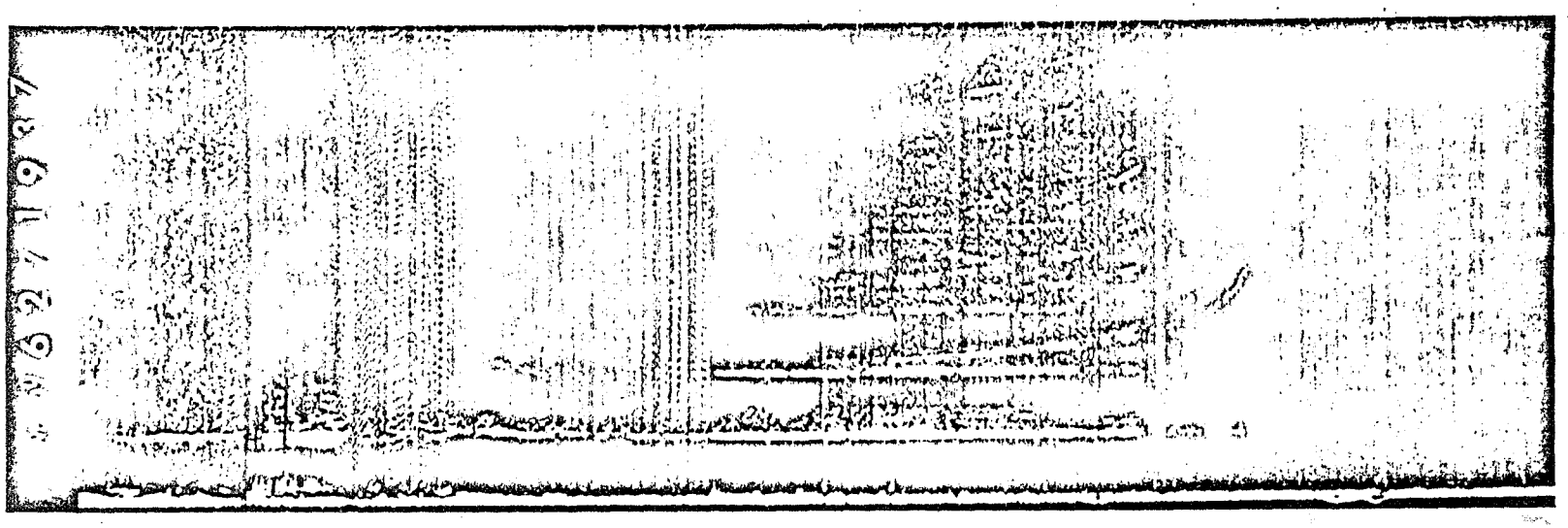

Figure 8 Ionogram two minutes after Launch

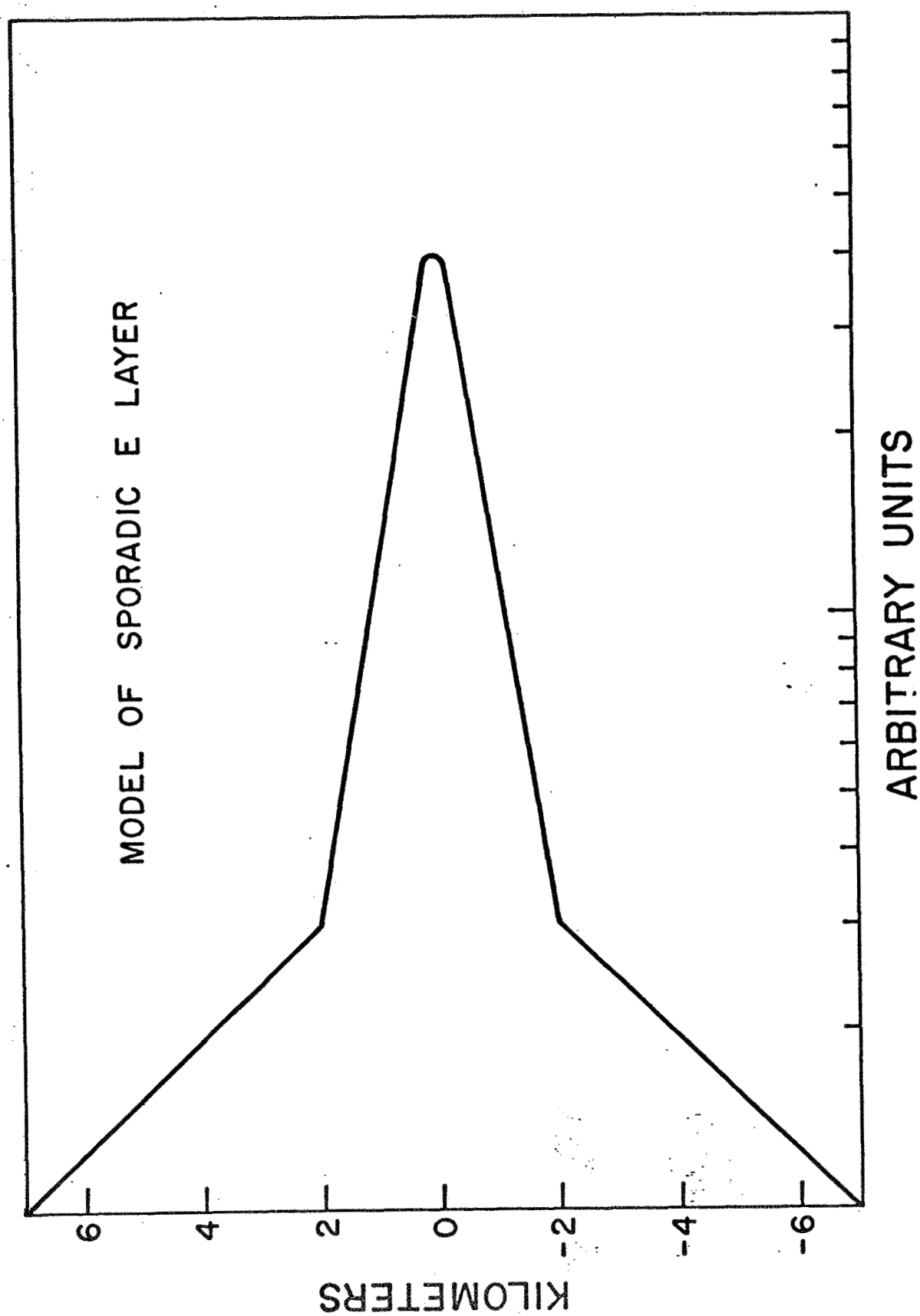

Figure 9 Model of MgII Layer

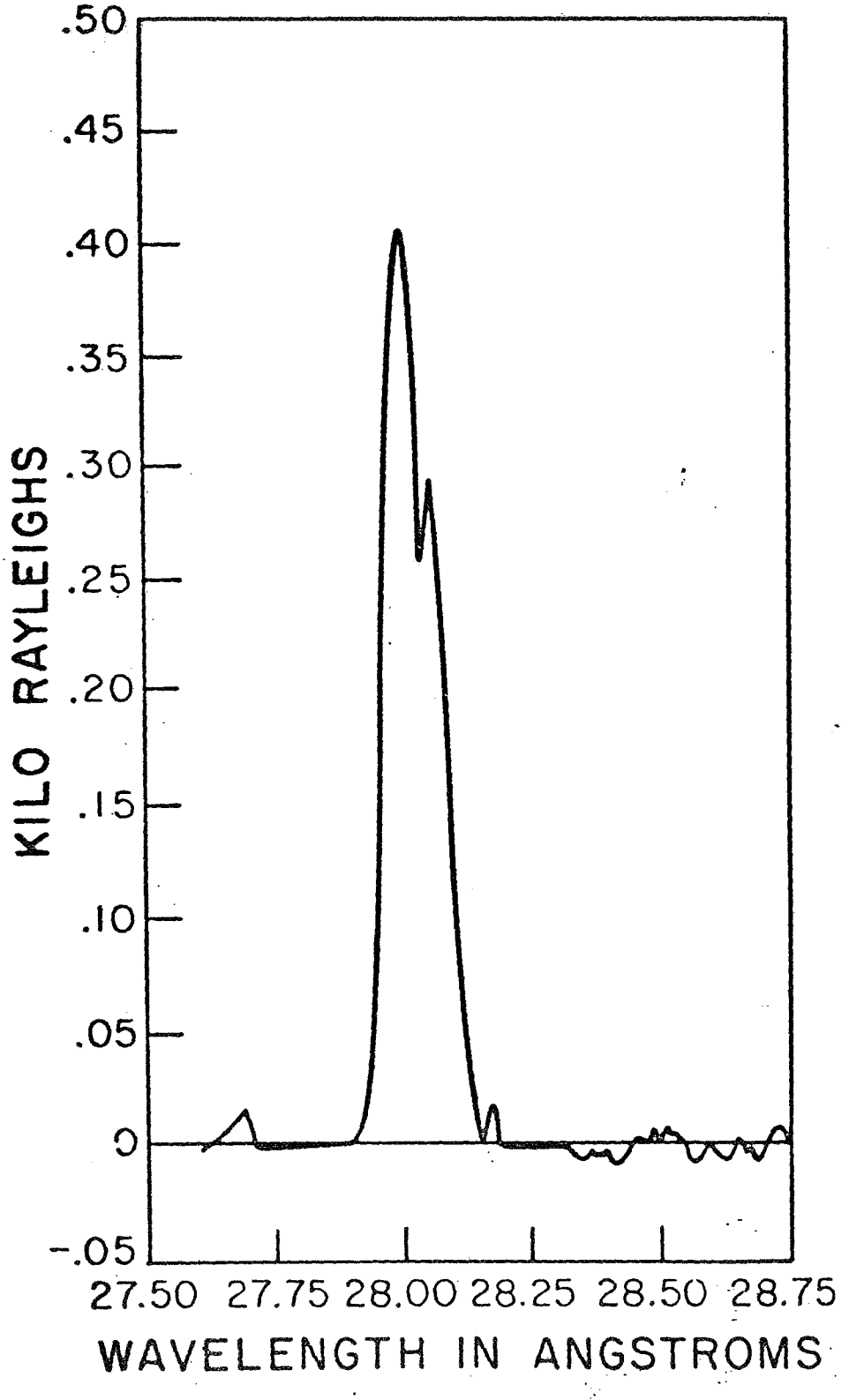

Figure 10 Sum of All Data Taken Showing Recognizable MgII Signal.

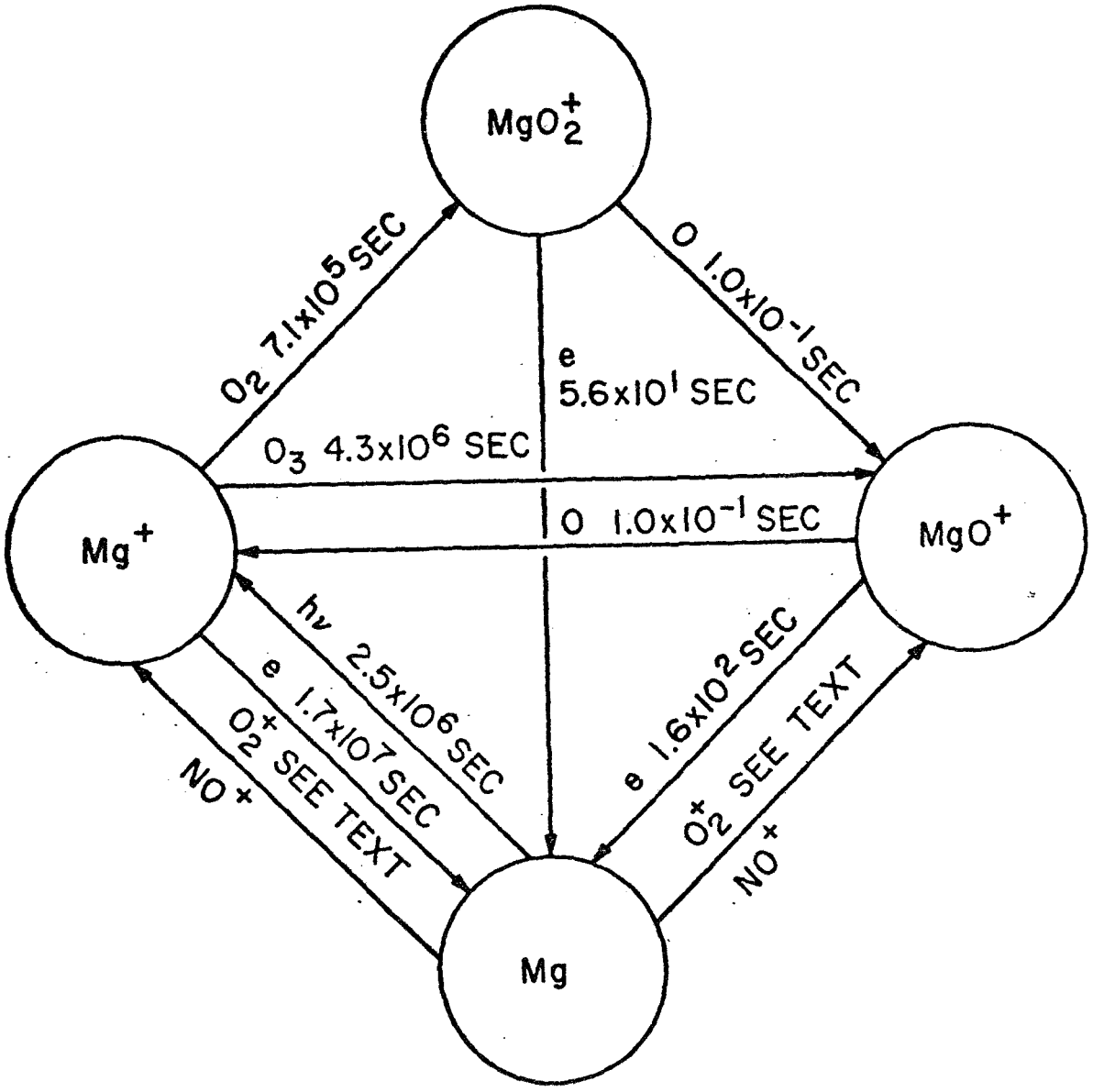

Figure 11 Schematic of Reaction Scheme